34th Annual International Conference of the IEEE EMBS
San Diego, California USA, 28 August - 1 September, 2012

Electrode Robustness in Artificial Cerebrospinal Fluid for Dielectrophoresis-based LoC

Mohamed Amine Miled[1], *Student Member, IEEE,* and Mohamad Sawan[1], *Fellow, IEEE*

***Abstract*— In this paper, we present hybrid microelectronics / microfluidic Lab-on-Chip (LoC) platform intended for implantable medical microsystems for neurotransmitter detection. In vitro experiments were achieved using artificial cerebrospinal fluid (ACSF) from Tocris Bioscience where microspheres were immersed to test the behaviour of the designed LoC. One of main features of the proposed LoC platform is its thin thickness, including micro-channels and silicon CMOS chip. The latter is integrated into the glass top-layer of the LoC measuring 0.5 mm. The size of the device is 9 mm × 5 mm. the electrode architecture is composed of 8×2×2 L-shaped electrodes in a 650 µm channel width and 4 sites for interdigitited electrodes . 32 L-shaped electrodes were connected to a electronics circuit for cells manipulation using dielectrophoresis (DEP). The described LoC achieved an efficient separation within a concentration of 50 µl of a solution of microspheres, distilled water (DW) and 500 µl of ACSF. Beyond this concentration, electrode destruction was observed.**

I. Introduction

It has been proven that the use of deep electrode for stimulation or detection for a bioimplant in the brain area induces a brain adaptation after few weeks of being implanted which has an impact on quality of either the detected or injected signal [1], [2]. In fact giant cells tend to grow in the peri-electrode space and are attached to the electrode [1]. The latter has low conductivity, which induces inaccurate measurement which is called electrode brain interface (EBI). This brain reaction interferes with sensing signal and results on a short-cut between electrodes as confirmed by Yousif et al who had shown that square pulse amplitude and shape is modified due to the EBI [1].

However, brain liquid can affect any implantable device or some part of its components due to ion or cell concentration. While, with the emerging packaging techniques, LoCs are becoming attractive to build implantable electronic devices and provide a viable solution to previously described problems. Despite this advancement, there are numerous drawbacks that need to be addressed to achieve a completely autonomous LoC-based implant. In addition, LoC packaging process has several fabrication constraints, such as microelectronics sensitivity and electrical protection, fluid injection, and mechanical aspects.

Consequently, different techniques have been proposed to package LoC devices [3], [4] to address issues like liquid leakage or pressure for wide range of applications and especially in the biomedical field.

[1]A. Miled and M. Sawan are with Ecole Polytechnique de Montreal, Electrical Engineering department, Montreal, Canada med-amine.miled@polymtl.ca

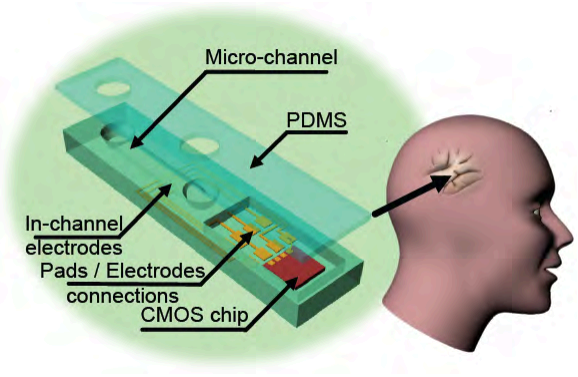

Fig. 1. Lab-on-Chip bioimplant proposed platform

Thus, in this work we propose a new approach, which consists of a fully integrated DEP-based lab-on-chip where the electrodes are embedded into a micro-channel and brain liquid is sampled and injected through this micro-channel for analysis as shown in Fig. 1. The proposed platform includes a microelectronics chip, and a microfluidic device. Both parts are packaged using glass and PDMS then they will be integrated into a biocompatible structure. The advantage of using DEP then other techniques is mainly because it is a label-free technique and does not need any preparation for cells or molecules. Thus, the presented system is dedicated to neurotransmitters detection and manipulation, and consequently, its final use will be as an implant that bestows special care on connections between microelectronics part and microfluidic channels. In Section II, the proposed design is described. Experimental results are shown in Section III, followed by a discussion. Finally, a conclusion highlights the main contribution and results.

II. IC/Microfluidic System Description

In order to describe the proposed LoC architecture, the microfluidic structure is first introduced, then the microelectronic part is elaborated.

A. Microfluidic Architecture

The microfluidic architecture has been designed for particles separation and detection using dielectrophoresis (DEP) [5] with a volume of 2 pl, which is the minimum that can be done with designed microfluidic architecture. In fact due to the limited available space in the cortex area and the liquid flowing between neurons, the sampling volume is a critical issue in the proposed design. Then, to reduce the amplitude of the applied voltage, an array of electrodes has been used.

978-1-4577-1787-1/12/$26.00 ©2012 IEEE

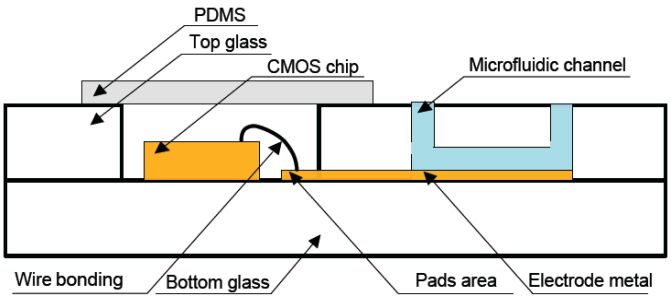

Fig. 2. Proposed LoC design based on two glass plates and a CMOS chip

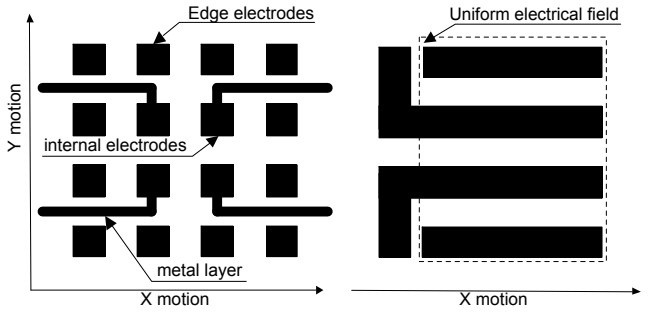

Fig. 3. Electrode configurations: (a) Square electrode array, (b) L-shaped electrodes

The area of each electrode is 10 µm × 10 µm. Using such small dimensions is required to employ a very narrow width of the channel where DEP forces, known as capillary DEP, are applied [6]. Thus, the channel length was reduced to 3 mm and the width to 650 µm. The microfluidic structure was fabricated with two borofloat glass plates. The micro-channel was designed on the top plate, while the electrodes with a thickness of 200 nm were located on the bottom plate. The same electrode metal with identical thickness was used to connect the electrical pads to them.

Furthermore, different investigations were carried out to determine the best electrodes design for cells manipulation [7], [8]. The main problem with regard to square electrodes is the connection to the CMOS chip. If the electrodes are integrated directly on the CMOS chip, then there is a limitation in the size of the cells to be manipulated and detected, which is related to the size of the microelectronics die. In addition, any problem affecting the microelectronics part or the microfluidic architecture implies replacement of all systems, which can be expensive and not useful for implants when the microfluidic architecture is complex. Thus, the best solution is to keep each part separated from the other. Square-array electrodes offer good configuration and achieve good electrical field propagation [9]. However, when using two glass plates to fabricate the microfluidic structure with only one metal layer, it is becoming hard task to connect all the electrodes to the microelectronics system directly. Thus, a routing path must be designed through electrodes to connect them. When the dimensions of the square electrodes are few micrometers, such as 10 µm × 10 µm and the distance between the two electrodes is 10 µm, then the routing path passing through them introduces a parasitic field and the electrical field may completely be out of control. Thus, a new electrode configuration known by L-shaped electrodes is introduced, as shown in Fig. 3.

However, due to the L-shaped electrode size and configuration, it is not appropriate to design them on the top layer of the CMOS chip. In fact, as the architecture includes 32 L-shaped electrodes, the area of the microfluidic structure is 650 µm × 650 µm. Uncovering such a big area on the CMOS chip keeps the electronic circuit unprotected from liquid leakage. Furthermore, to connect the electrodes to the IC, a complex array must be designed. These constraints reduce the number of metal layers needed for the electronic design in the IC, which is an important drawback for complex design requiring the use of all CMOS metal layers. Moreover, in this case, the microfluidic architecture is limited to the IC area. Thus, the L-shaped electrodes were designed and fabricated on the bottom plate of the microfluidic glass substrate.

The use of this configuration is a compromise to have a better control. In fact, by implementing a square-array electrode matrix, the electrical field propagation is controlled in X and Y directions, as shown in Fig. 3a. However, this is not the case owing to the presence of the routing path to connect the electrodes to the pads. Using the L-shaped electrodes, the electrical field is completely controllable through Y direction, which is sufficient for particle selection if they are injected in X direction with a constant speed.

B. Microelectronics Integrated Circuit

As the proposed LoC is specifically designed for particle manipulation and detection, the microelectronics chip generates and controls the required electrical field [10]. In fact, each L-shaped electrode will propagate an electrical field dephased by 180° when compared with the previous electrode. In this way, the particle manipulation relies on the dimension and the weight of target particles. Depending on the signal amplitude, particles with greater weight than others assays will be trapped by some electrodes and those with lower weight will be captured by others. Thus, the microelectronics chip can generate a variable amplitude voltage and then dispatch it onto the target electrodes.

III. Experimental Results

The microfluidic architecture has a 1 mm thickness (Fig. 4). It is composed of two different glass layers. The thickness of each layer is 0.5 mm. The depth of the micro-channel was 25 µm and its width was 650 µm. The L-shaped electrodes were made with Au-Pt metal layer. Their width was 10 µm and the distance between two successive electrodes was 10 µm. The length of the electrodes in the uniform electrical field area presented in Fig. 3 was 2 mm, and the diameter of the access of a single hole was 1.5 mm. These dimensions are the minimum, that were allowed by Leonix, and the electrodes were connected to the pads made by the same Au-Pt layer and then to the CMOS chip (Fig. 4b).The microelectronics part is designed using CMOS TSMC 0.18 µm technology and it is shown in Fig. 4b. For practical

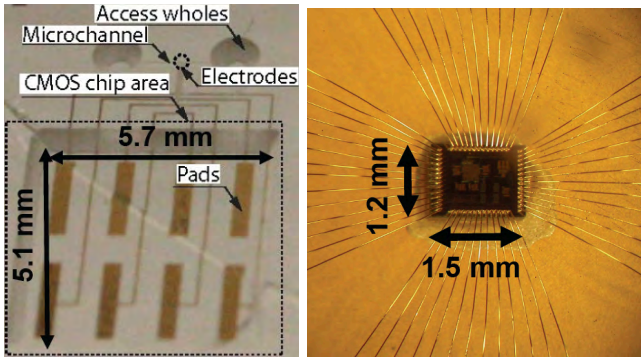

(a) (b)

Fig. 4. IC assembly: (a) microfluidic structure, and (b) microelectronics CMOS chip

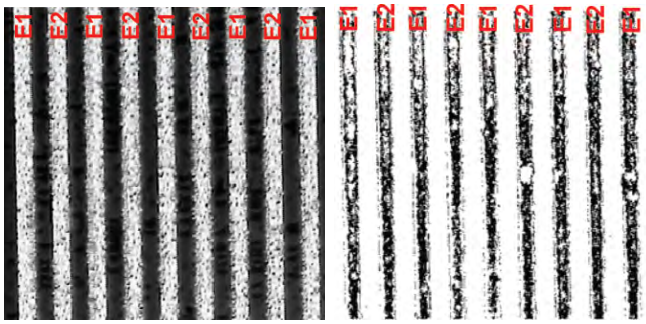

(a) (b)

Fig. 5. Separation of PC05N and PS03N polymer microspheres with L-shaped electrode architecture: (a) PC05N (black stripes in inter-electrode space) and PS03N (gray particles on white electrodes) at low frequency 4.8 kHz, (b) PC05N immobilized on electrodes surfaces and PS03N dissipated due to transportation effect at high frequency 1.25 MHz

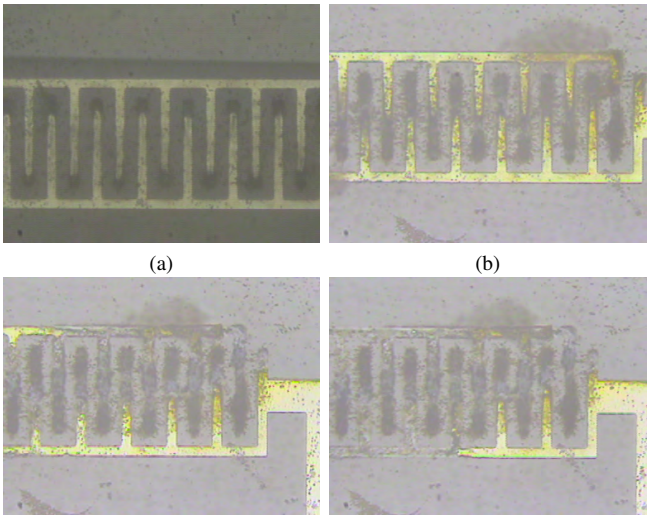

(a) (b) (c) (d)

Fig. 6. Electrode disintegration when exposed to ACSF (a) before applying electrical any electrical field and after (b) 0 min, (c) 3 min, (d) 13 min

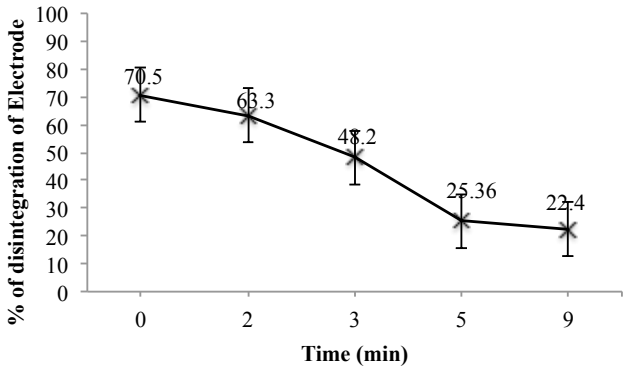

Fig. 7. Impact of 400 µl ACSF within 1.8 ml of DW with 40 µl of 1 µm microspheres on electrode.

reasons, the output signal from the CMOS chip was amplified to test the platform with different microsphere weights.

All experiments where performed using a sinusoidal AC signal, and the application of a phase shift of 0° on electrode 1 (E1) and 180° electrode 2 (E2) to each pairs of electrode. The frequency was swept from 900 Hz to 1.25 MHz, the lowest value was chosen in order to prevent the formation of chemical reactions and bubbles.

First, the LoC electrode architecture and fabrication was tested with ACSF to find the suitable buffer solution. In fact when injecting the ACSF solution directly into microchannels and as soon as an electrical field is applied all electrodes are completely disintegrated. For testing purpose, a solution composed of 400 µl ACSF within 1.8 ml of DW with 40 µl of 1 µm microspheres on electrode was injected inside the microchannel. A partial disintegration of electrodes was observed from the beginning until reaching a highly disintegration of around 80 % of the electrode as shown in Fig. 6 and 7. However, from 20 % of disintegration the DEP effect is considerably reduced. Thus, a buffer solution must be added to the ACSF to achieve an efficient DEP separation while preserving electrode architecture.

Various concentrations of ACSF were tested with a buffer solution of 500 µl DW. It was observed that from 30 µl of ACSF electrode disintegration becomes more considerable and DEP effect is considerably reduced. However, the cross-frequency defining the change from nDEP to pDEP is slightly affected by ACSF concentration. In fact, DEP moves from pDEP to nDEP between 6 kHz and 9.6 kHz as shown in Fig. 8 and 9 for various concentration of ACSF between 5 µl and 30 µl.

Two types of negative-charge polymer microspheres were used to distinguish the different observed phenomena. The first one are made of polystyrene PS03N from Bangs laboratories and have a 2.04 µm diameter, while the second type consists of carboxyl-functionalized polystyrene PC05N from Bangs laboratories too and have a 0.51 µm diameter. The polymer beads were diluted in deionized water to create a solution with a final concentration of 0.8 $\mathrm{mg/ml}$ to 2 $\mathrm{mg/ml}$.

First, qualitative observations on DEP of PS03N and PC05N microspheres at various frequencies are made for both types of electrode architectures. Visual observations under a microscope show a transition of pDEP to nDEP at a precise frequency value which is specific to the type of microspheres and independent of the used electrode configuration. This transition was detected at a frequency of 9 kHz for PS03N microparticles and of 627 kHz for PC05N

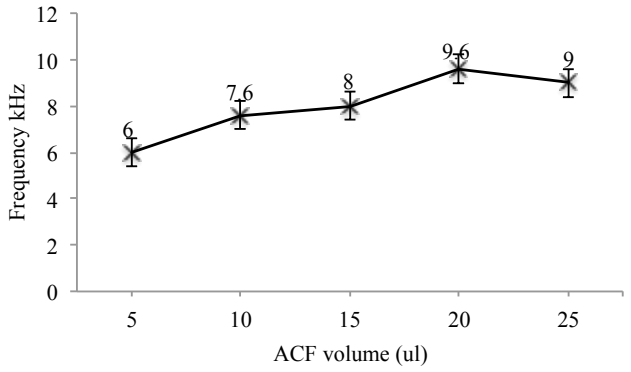

Fig. 8. Variation of DEP change frequency versus various solution of ACSF in 500 µl of DW

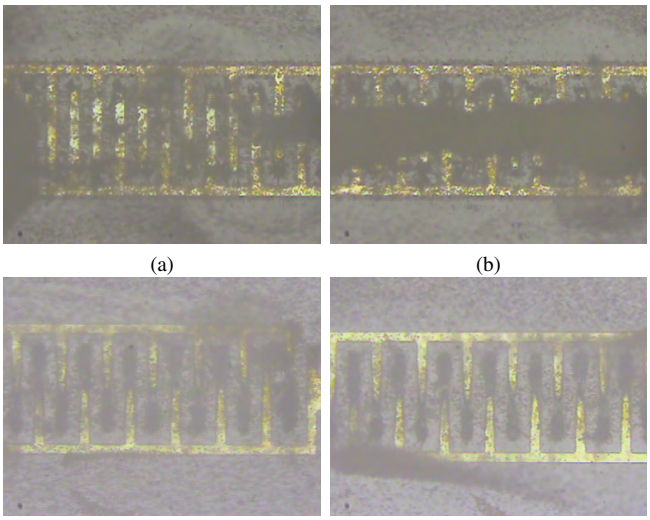

Fig. 9. DEP effect for various concentration of ACSF: (a) and (c) show nDEP when 5 µl and 30 µl of ACSF are injected with 500 µl of DW respectively; (b), and (d) show a pDEP effect for the same concentrations respectively

microparticles.

The separation operation relies on the fact that PS03N has unique frequency-dependent dielectric properties, different from PC05N. Particles are initially observed under the microscope separately and then together. At low frequencies, PS03N polymer microspheres are attracted to the electrode surfaces, while they are repelled at a frequency greater than 9 kHz. PC05N polymer microspheres show a more complex behavior. At low frequency, particles form stationary aggregates and perpendicular to the direction of the electrodes and they are located in the inter-electrodes space. At a frequency greater than the pDEP to nDEP transition frequency, 627 kHz, the PC05N particles are attracted to the electrode surface where they become immobilized. The same behaviors visualized individually have been separately identified when a mixture of both types of polymer microspheres in equal proportions was conducted and analyzed qualitatively in Fig. 5, validating our system ability to separate particles of different nature.

IV. Conclusion

We have presented a new packaging process for CMOS chip, microfluidic architecture, and PDMS tubing in the same platform. The packaging was successfully realized and all the systems were encapsulated inside 10 mm × 5 mm area and 2 mm thickness. The LoC included micro-channels designed onto two glass plates and bonded together based on a commercial process. The CMOS chip was glued onto the topside of the bottom plate where the corresponding side of the top plate was cut off. The system has been designed for small particles in the range of nanometres, and tested with 500 nm and 2 µm micro-spheres by applying a sinusoidal signal whose amplitude was variable from 3 to 6.6 V on ACSF. As it is on going project, future works are targeting a fully automated system with auto-calibration for a better detection of micro and nano particles [10].

ACKNOWLEDGMENT

The authors acknowledge the financial support from NSERC and Canada Research Chair in Smart Medical Devices, and are grateful for the design and simulation tools supplied by CMC Microsystems.

References

[1] N. Yousif, R. Bayford, and X. Liu, "The influence of reactivity of the electrode-brain interface on the crossing electric current in therapeutic deep brain stimulation," *J. Neuroscience*, vol. 156, no. 3, pp. 597 – 606, 2008.

[2] J. R. Wolpaw, N. Birbaumer, D. J. McFarland, G. Pfurtscheller, and T. M. Vaughan, "Brain-computer interfaces for communication and control," *Clinical Neurophysiology*, vol. 113, no. 6, pp. 767 – 791, 2002.

[3] R. Thuenauer, K. Juhasz, R. Mayr, T. Fruhwirth, A.-M. Lipp, Z. Balogi, and A. Sonnleitner, "A pdms-based biochip with integrated sub-micrometre position control for tirf microscopy of the apical cell membrane," *Lab Chip*, 2011.

[4] E. R. Murphy, T. Inoue, H. R. Sahoo, N. Zaborenko, and K. F. Jensen, "Solder-based chip-to-tube and chip-to-chip packaging for microfluidic devices," *Lab Chip*, vol. 7, pp. 1309–1314, 2007.

[5] S. Masuda and T. Kamimura, "Approximate methods for calculating a non-uniform travelling field," *J. electrostatics*, vol. 1, no. 1, pp. 351–370, 1975.

[6] H. Becker, K. Lowack, and A. Manz, "Planar quartz chips with submicron channels for two-dimensional capillary electrophoresis applications," *J. Micromech. Microeng.*, vol. 8, no. 1, pp. 24–28, 1998.

[7] D. Padmaraj, W. Zagozdzon-Wosik, L.-M. Xie, V. G. Hadjiev, P. Cherukuri, and J. Wosik, "Parallel and orthogonal e-field alignment of single-walled carbon nanotubes by ac dielectrophoresis," *J. Nanotechnology*, vol. 20, no. 3, p. 035201 (7pp), 2009.

[8] M. Miled, A. Gagne, and M. Sawan, "Electrodes architectures for dielectrophoretic-based cells manipulation in locs: Modeling, simulation and experimental results," in *Mixed-Signals, Sensors and Systems Test Workshop (IMS3TW), 2011 IEEE 17th International*, May. 2011, pp. 39 –42.

[9] G. Medoro, C. Nastruzzi, R. Guerrieri, R. Gambari, and N. Manaresi, "Lab on a chip for live-cell manipulation," *IEEE Des. Test of Comput.*, vol. 24, no. 1, pp. 26–36, Jan. 2007.

[10] M. Miled and M. Sawan, "Dielectrophoresis-based integrated lab-on-chip for nano and micro-particles manipulation and capacitive detection," *IEEE Trans. Biomed. Circuits. Syst.*, vol. 6, no. 2, pp. 120 –132, Apr. 2012.